AEDC-TR-71-163

cy 2

FREQUENCY BROADENING IN REFERENCE BEAM LASER DOPPLER VELOCIMETER DATA

W. H. Goethert

ARO, Inc.

September 1971

ARNOLD ENGINEERING DEVELOPMENT CENTER
AIR FORCE SYSTEMS COMMAND
ARNOLD AIR FORCE STATION, TENNESSEE

NOTICES

When U. S. Government drawings specifications, or other data are used for any purpose other than a definitely related Government procurement operation, the Government thereby incurs no responsibility nor any obligation whatsoever, and the fact that the Government may have formulated, furnished, or in any way supplied the said drawings, specifications, or other data, is not to be regarded by implication or otherwise, or in any manner licensing the holder or any other person or corporation, or conveying any rights or permission to manufacture, use, or sell any patented invention that may in any way be related thereto.

Qualified users may obtain copies of this report from the Defense Documentation Center.

References to named commercial products in this report are not to be considered in any sense as an endorsement of the product by the United States Air Force or the Government.

FREQUENCY BROADENING IN REFERENCE BEAM LASER DOPPLER VELOCIMETER DATA

W. H. Goethert
ARO, Inc.

FOREWORD

The work reported herein was sponsored by Headquarters, Arnold Engineering Development Center (AEDC), Air Force Systems Command (AFSC), under Program Element 64719F, Project 4344.

The results of this research were obtained by ARO, Inc. (a subsidiary of Sverdrup & Parcel and Associates, Inc.), contract operator of AEDC, AFSC, Arnold Air Force Station, Tennessee, under Contract F40600-72-C-0003. The research was performed under ARO Project No. BC5019, and the manuscript was submitted for publication May 24, 1971.

The author wishes to acknowledge Mr. H. J. Parsons for his invaluable assistance in fabrication of the associated hardware and Mr. E. B. Harding for assisting in the data acquisition.

This technical report has been reviewed and is approved.

David G. Francis
Captain, USAF
Research and Development Division
Directorate of Technology

Robert O. Dietz
Acting Director
Directorate of Technology

ABSTRACT

The laser Doppler velocimeter (LDV) provides velocity data in the form of a frequency spectrum. Because of the inherent optical geometry of the laser velocimeter and the effects of light scattering particles passing through the probe volume, a frequency distribution density function representing these combined effects is found in the readout device. Hence, interpretation of data must be effected for frequency-to-velocity conversion. This report deals with this frequency broadening effect associated with the LDV reference beam type. Six frequency broadening effects are discussed in terms of their magnitude and relative importance.

CONTENTS

		Page
	ABSTRACT	iii
I.	INTRODUCTION	1
II.	THE LASER DOPPLER VELOCIMETER TECHNIQUE	1
III.	FREQUENCY SPECTRUM ANALYSIS	2
IV.	FREQUENCY BROADENING	
	4.1 Aperture Broadening	3
	4.2 Effect of Δk_s and Δk_o	7
	4.3 Transient Doppler Data	11
	4.4 Frequency Modulation	12
	4.5 Brownian Motion	13
V.	SUMMARY AND CONCLUSION	18
	REFERENCES	19

APPENDIXES

I. ILLUSTRATIONS

Figure

1.	Schematic Diagram of Flow System	23
2.	Setup of the LDV on the Water Flow System	24
3.	Frequency Broadening at Constant Settings of Readout Instrument at Various Stations of the Channel Flow	25
4.	Model of Scattering Volume	26
5.	Normalized Velocity Profile	27
6.	Velocity Gradient Projection	
	a. Nonlinear Velocity Gradient Projected into the Frequency Domain	28
	b. Almost Linear Velocity Gradient Projected into an Almost Gaussian Frequency Distribution	29
7.	Boundary Layer Frequency Distribution	30
8.	Vector Representation of the Velocity Measurement	31
9.	Amplitude-Frequency Variation	32
10.	Effects of Frequency Modulation	33

Page

II. TABLES

I. Calculated and Experimental Maximum Intensity 34

II. Summary of Broadening Effects. 35

SECTION I
INTRODUCTION

The laser Doppler shift velocimeter has been developed within the laboratory to obtain accurate velocity measurements of flowing liquids and gases. It is generally assumed that the volume element in which the fluid velocity is being measured is small. Under these conditions, a unique frequency might be expected on the spectrum analyzer display. This, of course, would assume laminar, nonfluctuating flow. Unique frequencies (velocities) have been experimentally approached in laminar water flow. However, extreme care had to be taken to eliminate problems in the flow systems such as air pockets and air bubbles trapped in the flow loop, in addition to isolating the water pump with the use of a "water tower" technique, thereby obviating any pressure surges. Such a flow loop is shown in Fig. 1, Appendix I (Ref. 1).

During the course of the experimental work, it was found that signal broadening was generally evidenced on the spectrum analyzer. It was originally assumed that any departure from a sharp signal frequency display to a broadened signal could be attributed to some form of turbulence. In actuality, however, there are several additional contributions for broadening of the frequency spectrum. The objective of this report is to discuss the causes and nature of frequency broadening in detail. A model of the scattering volume is formulated, and the distribution function as obtained from a spectrum analyzer is evaluated and compared with the experimental data taken from the flow channel illustrated in Fig. 1.

SECTION II
THE LASER DOPPLER VELOCIMETER TECHNIQUE

The velocity at any point in the flow field may be determined by measuring the Doppler shifted signal stemming from the interaction of a monochromatic laser light source with seed particles in the fluid. The seed particles are necessary because of their large scattering cross section and small thermal velocities compared with gas or liquid particles. Scattered light from the seed particles and light from a reference source are combined by means of an optical heterodyne technique, and the resulting Doppler frequency is measured by a photomultiplier. The frequency of the photodetector output can be shown to be related to velocity of the flowing fluid by the following expression:

$$f_D = \frac{1}{2\pi}(\bar{k}_s - \bar{k}_o) \cdot \bar{v} \tag{1}$$

where

$$\bar{k}_s = \frac{2\pi}{\lambda} n\tilde{e}_s$$

$\bar{v}$ is the velocity vector of the fluid flow, f_D is the Doppler shifted frequency, and $\bar{k}_S$ and $\bar{k}_O$ are the propagation vectors of the scatter and reference laser beam, respectively. The propagation vector is a function of the index of refraction n, the wavelength λ, and the unit vector $\tilde{e}_S$ in the s direction. The LDV setup on the water flow system is schematically illustrated in Fig. 2, where the light source is a Spectra-Physics Model 122 helium-neon laser having 3 mw of coherent light power. The experimental arrangement shown in Fig. 2 can be mathematically resolved into the following expression:

$$f_D = \frac{nv_x}{\lambda_o} \sin\theta = c_1 v \tag{2}$$

where c_1 is a constant, n the index of refraction of the scattering medium, λ_O the wavelength of the coherent light source, and θ is the angle between the reference beam and the direction of the scattered light. From Eq. (2) it can be readily seen that once the geometry is fixed, θ is known; the wavelength of the monochromatic laser source is known; the index of refraction is known, and therefore, the velocity is directly proportional to the Doppler frequency. Hence, in any subsequent discussions the velocity and the Doppler frequency can be freely interchanged.

SECTION III
FREQUENCY SPECTRUM ANALYSIS

In the ideal case of a Doppler frequency, continuous in time, the frequency is detected, amplified, and displayed in some suitable fashion. This ideal condition is not generally found in practice; hence, a more realistic frequency analysis is required. If the detected Doppler frequency is continuous in time and sinusoidal in form, it may be expressed mathematically by a time-varying function as follows:

$$x(t) = X \sin(2\pi f_o t + \tau)$$

where X is the maximum amplitude, f_O is the frequency, and τ is the phase in radians. The signal may be displayed either as x(t) describing the time history as above or as a display of the frequency domain of the detected signal. Generally, deterministic data are in complex periodic form that may be expressed as a combination of noncontinuous sinusoidal

wave trains with appropriate amplitudes. The detected Doppler shifted frequencies may be displayed in the frequency domain in accordance to the various velocities contributing to the signals received by the phototube. The spectrum analyzer is a device that displays the frequency content (or velocities) present in the light collected at the phototube. This display closely represents the distribution density function. There are electronic limitations in the conversion from the time domain to frequency domain such that some reference must be made for accurate interpretation of this frequency display (Ref. 2). Some of these limitations will be discussed in a later section dealing with Doppler frequency broadening due to transient data.

SECTION IV
FREQUENCY BROADENING

4.1 APERTURE BROADENING

Frequency broadening, due to the projection of the aperture onto the focal volume in the flow field, will be considered assuming all other broadening effects are negligible. The origin for this study arrived from the frequency broadening in the boundary layer of the water flow channel depicted schematically in Fig. 1. It was generally believed that a form of boundary layer turbulence may be taking place which would, indeed, produce frequency broadening. Figure 3 illustrates typical frequency displays of the constant velocity in the center of the test section, the broadening effects observed at "just in" the boundary layer, and the large broadening effect near the wall of the test section. These photographs illustrate typical broadening effects in LDV systems which clearly indicated the need for accurate interpretation of the displays.

4.1.1 Origin of Aperture Broadening Effects

Figure 2 illustrates the optical setup where the velocities are measured at point V determined by the focal point of a laser beam system. The spot size, limited by the resolving power of the lens, is determined at the $1/e^2$ intensity points, for a Gaussian intensity distribution by

$$D = \frac{4f\lambda}{\pi a} = 1.273\,\frac{f\lambda}{a} \tag{3}$$

where D is the resulting spot diameter, f is the focal length of the lens, λ is the wavelength of the light being focused, and a is the diameter of the light beam entering the focusing lens. Figure 4 illustrates this

minimum diameter, or diffraction limited laser light beam, at the focal point. An approximate normalized intensity distribution at the minimum focused diameter is also shown in the figure. It can be shown (Ref. 3) that the intensity distribution in the focal spot may be closely approximated by a Gaussian intensity distribution for a laser operating in the fundamental mode.

In general, the amount of light contributing to the Doppler shifted signal is determined by the receiving optics. A scattered beam collecting lens (Fig. 2) is used for imaging the light scattering volume on an aperture slit preceding the photomultiplier tube. The aperture size determines the amount of light to be collected from the scattering volume, as illustrated in Fig. 4. This finite width of the aperture slit also determines the portion of the scattering volume that is sampled. The aperture slit dimension is generally set at an opening of at least 0.5 mm or greater to avoid losses due to Fresnel diffraction. With this fixed slit width, a velocity profile was obtained in the entrance region[1] of the parallel plate water channel. A velocity profile was taken across the channel at a point where both a region of constant velocity and a constant velocity gradient (due to the developing wall boundary layer) was evident. Figure 5 contains a plot of the normalized velocity profile from the center of the channel to the wall. The spectrum analyzer displays were photographed at the channel position indicated. The image of the light scattering volume could be converted to the flow channel dimension by noting channel wall position in the image. Since the channel width was known accurately, the ratio of aperture slit to channel width was calculated. In this manner, it was possible to determine the effective width of the aperture at the point where measurements were made. The bands are placed on the velocity profile curve of Fig. 5 at the location in the channel where the measurements were made.

The finite width of the aperture sampling a finite portion of the flow field is manifested in the spectrum analyzer display and will be referred to here as the density function. The density function displayed on the spectrum analyzer originated from the total frequency content in light collecting configuration. It is easily verified that a constant velocity in this first approximation corresponds to one frequency, Eq. (2). Therefore, by assuming an ideal instrument, the display consists of a single vertical deflection corresponding to the constant velocity which is independent of the scattered light intensity distribution.

---

[1]The entrance region is the transition region from a flat velocity profile created by a diffuser screen, seen in Fig. 1, and the fully developed Poiseuille flow region.

In the case when there is a linear change in velocity versus position within the aperture limits, all frequencies corresponding to these velocities will be present in the spectrum analyzer display. Figure 4 shows the effect of the scattered light intensity distribution corresponding to velocities throughout the projected aperture slit. The velocities present at the periphery of the laser beam scatter very little light, where in the center of the laser beam, maximum light intensity is being scattered to the detector.

Since velocity gradients are present in the boundary layer of the flow field and change with position, each gradient must be treated separately. Two representative figures depicting velocity gradients are plotted in Fig. 6 to show their effects in the frequency domain. The velocity limits of these plots indicate the finite width of the aperture slit such that Fig. 6 represents Fig. 5 in the appropriate channel position. The intensity distributions (Fig. 4) provide for the maximum scattering intensity to emanate from the geometrical center of the scattering volume; hence, the geometrical center of these velocity distributions may be established as the maximum or predominant velocity of the distribution density function. The method used for determining the density functions in Fig. 6 is as follows:

1. The limits of the velocity in Fig. 6a top are taken to be the zero amplitude points in Fig. 6a bottom.
2. The most dominant velocity is taken to be at the intersection of the geometrical center of the aperture and the velocity curve. Figure 6a top is taken to be the maximum amplitude point of Fig. 6a bottom.
3. A smooth curve is drawn between these three points such that, if the predominant velocity occurred in the center, a normal distribution density function could be drawn in its limits, and if the predominant velocity was found to one side of the center, a Rayleigh density function was used to describe the distribution. It is important to note that when the velocity is changing nonlinearly, that is,

$$\frac{d}{dx}\left[\frac{dv}{dx}\right] \neq 0$$

the density function becomes skewed to one side and may be described by a Rayleigh or Chi-squared density function. From Fig. 6 it is apparent that the skewness always tends towards the low velocity side. When

$$\frac{d}{dx}\left[\frac{dv}{dx}\right] = 0$$

then

$$\frac{dv}{dx} = \text{constant}$$

and the distribution density function becomes a normal distribution, also seen in Fig. 6.

4.1.2 Comparison with Experiments

Each light scattering volume (Fig. 6) has a corresponding frequency density function, as seen by the spectrum analyzer (directly proportional to velocity). All that needs to be done for comparison is to determine the relative amplitude of the density function determined in the previous section. The focal point intensity distribution may be approximated by a normal or Gaussian density function by

$$g(x) = \frac{1}{\sigma\sqrt{2\pi}} \exp -\left[\frac{(x-\mu)^2}{2\sigma^2}\right] \qquad -\infty < x < \infty \tag{4}$$

where σ is the variance given by

$$\sigma^2 = \int_{-\infty}^{\infty} (x-\mu)^2 \, g(x) \, dx$$

and μ is the position of maximum intensity. It is seen that the (velocity) frequency density function of the scattering volume has a similar, or proportional, distribution since the maximum scattered light has its origin in the center of scattered volume. To clarify this point, reference is made to Fig. 4. Consider an infinitesimal slit opening represented by a straight line in the direction of a collecting lens. A velocity gradient is imposed on the limits of the infinitesimal small slit width as shown in the figure. The light intensity versus position along this line is represented by the intensity curve shown perpendicular to the slit. The arrows under the envelope represent the corresponding scattered light intensity associated with that particular position. By assuming that on the spectrum analyzer trace each frequency corresponds to a particular position x such that with v being a linear function of f,

$$x \approx c_1 v$$

then

$$g(x) = g(c_1 v)$$

becomes a fair approximation. By assuming f(v) is Gaussian, then at the maximum, or predominant, velocity

$$f(v)_{max} = \frac{1}{\sigma\sqrt{2\pi}} \propto \frac{k}{b} \tag{5}$$

where b is determined by $V_{max} - V_{min}$ in the slit width indicated and k is the proportionality constant connecting the maximum intensity from the photographs to the calculated maximum intensity from the finite slit width. In this experiment, k was arbitrarily taken equal to one. Table I (Appendix II) is a tabulation of $f(v)_{max} \propto k/b$ and $\ell n\,(k/b)$ for each curve since the spectrum analyzer displayed the log of vertical deflections on the screen. A comparison of the experimental distribution density function and the density function determined in Section 4.1.7 is shown in Fig. 7. Excellent agreement is seen in both the boundary layer and in the nonboundary layer region, with the exception being in the very low velocity range where the velocity seems to flare out more than predicted. This variation was found to be due to low frequency vibrations of the optics table. Such vibrations appear as a vertical deflection in the low frequency domain. Hence, the so-called "boundary layer turbulence" may be entirely explained by velocity gradients in the finite slit width or field stop preceding the phototube.

4.2 EFFECT OF Δk_s AND Δk_o

As was pointed out previously, the focal spot diameter is a function of input diameter and focal length of the focusing lens or is functionally dependent on the solid angle of the light beam. Several $\bar{k}$ vectors are associated within the solid angle, such that $\Delta\bar{k}$ is taken as the angular variation in the propagation vector.

In reference to Eq. (1) which gives the Doppler frequency in terms of these vectors, the Doppler equation may be made more meaningful by changing the equation in terms of their appropriate unit vectors. Since

$$\bar{k}_s = \frac{n\,2\pi}{\lambda}\,\tilde{e}_s$$

where $\tilde{e}_s$ is the unit vector in the direction of $\bar{k}_s$ and

$$\bar{k}_o = \frac{n\,2\pi}{\lambda}\,\tilde{e}_o$$

and since

$$|\bar{k}_o| \cong |\bar{k}_s|$$

Eq. (1) may be written as

$$f_D = \frac{n}{\lambda}(\tilde{e}_s - \tilde{e}_o) \cdot \bar{v} \qquad (6)$$

This equation shows that the Doppler frequency is associated with the velocity component along $(\tilde{e}_s - \tilde{e}_o)$. Let $(\tilde{e}_s - \tilde{e}_o) = a\,\tilde{e}_y$. Figure 8 illustrates the unit vectors with appropriate spread determined by the solid angle subtended by each laser beam.

Two frequency broadening effects may be considered for Eq. (2) due to the spread in $\tilde{e}_o$ and $\tilde{e}_s$ vectors which are (see Fig. 8):

I. Broadening due to a variation in the direction of $\tilde{e}_y$.

II. Broadening due to a spread in θ.

4.2.1 Type I Broadening

(A) Consider the case where the velocity is constant and the LDV is geometrically oriented to measure along $\tilde{e}_y$ as shown

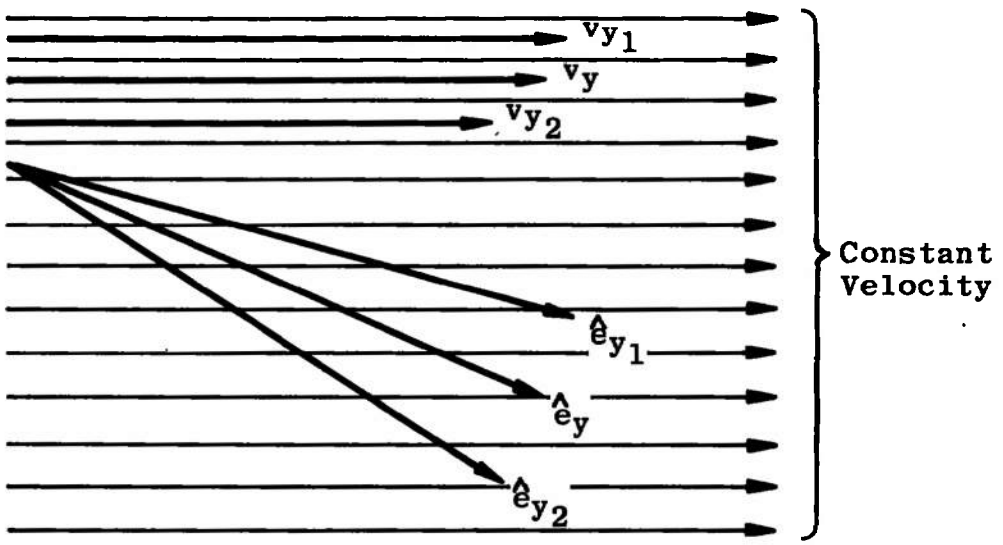

It is seen here that the dot product of the constant velocity v with $\tilde{e}_{y2}$ produces a lesser velocity component of v and $\tilde{e}_{y1}$ a greater velocity component of v (or $v_{y2} < v_y < v_{y1}$). This implies a nonsymmetric frequency broadening since the projection of the direction vectors, $\tilde{e}_y$, varies as the cosine. This is shown below.

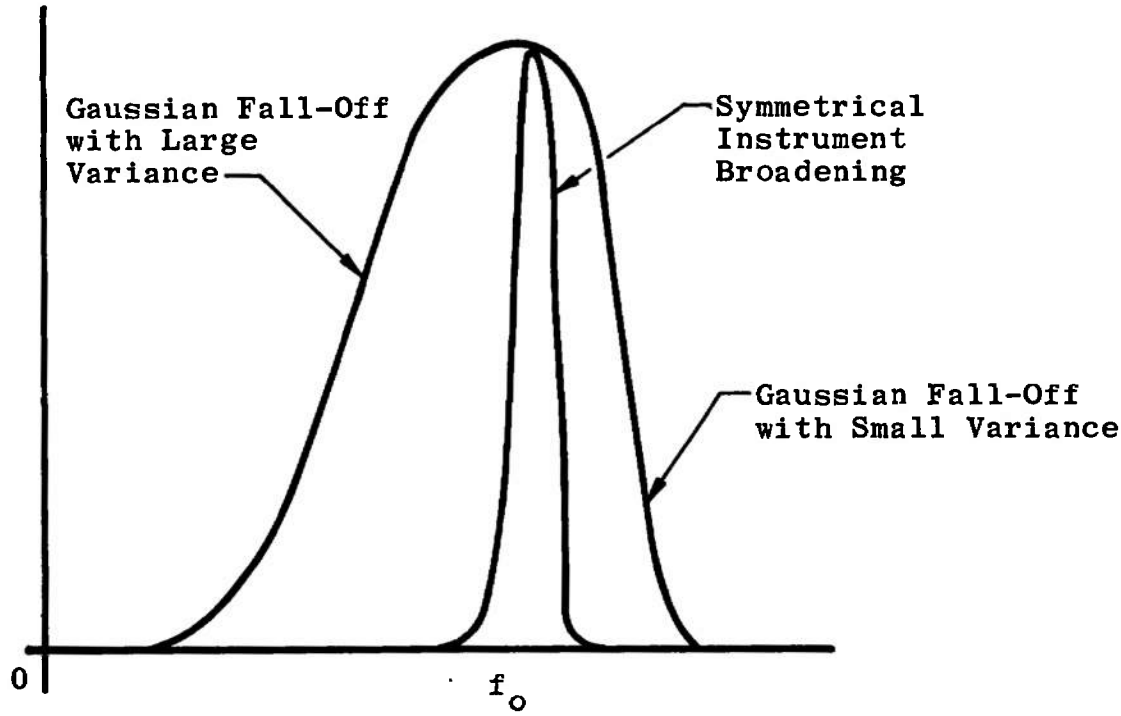

The higher frequency side of f_o falls off much more rapidly than the lower frequency side since the velocity components are a function of the cosine relations of the actual velocity.

(B) The other consideration is a special case of (A). Here $\tilde{e}_y$ is along the actual velocity v such that (v_{y2} and v_{y1}) < v_y. In this case, the frequency display would be as shown.

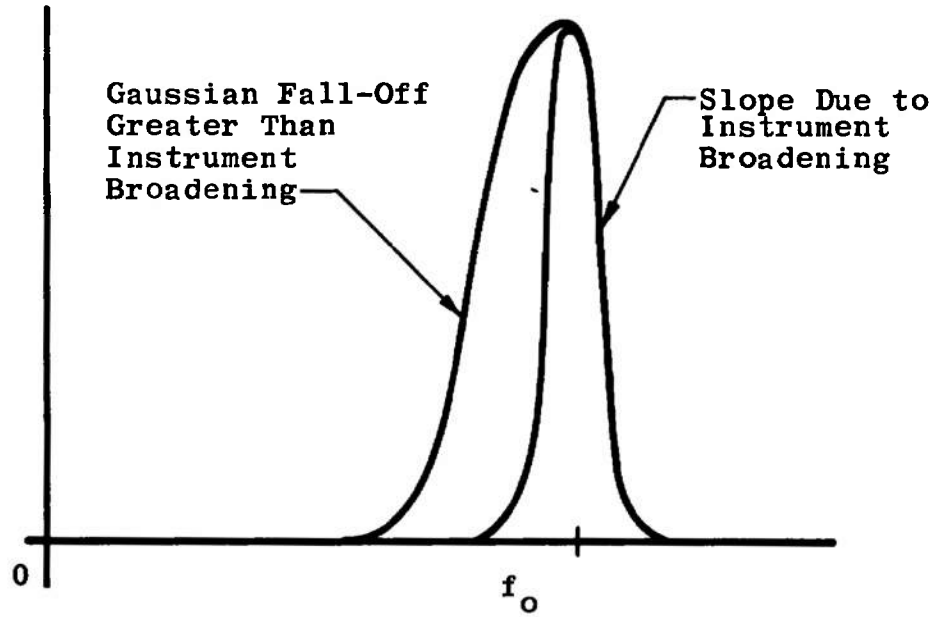

The case of Type I broadening with the angle between the incident beam and velocity vector known (angle 4) is now considered. In Fig. 8, α, β, and γ are defined. From geometrical considerations $\gamma = \frac{\alpha}{2} + \frac{\beta}{2}$. The values of α and β may be found from the f-number of each respective "beam." The f-number is defined as the focal length divided by diameter of the "beam"; hence the half-angle is β or $\alpha = \tan^{-1}\left(\frac{\text{diam}/2}{\text{focal length}}\right)$ or $\alpha = \tan^{-1}\left(\frac{1}{2f}\right)$ where f is the f-number. The Δv due to the variation in the direction vector $\tilde{e}_y$ is found to be

$$\Delta v_{\Delta e} = v\left[2 \cos\left(\frac{\theta}{2} + \psi\right) \sin \gamma\right]$$

To find Δf, the angle that produces this $\Delta v_{\Delta e}$ is used, i. e.,

$$\Delta f_{\Delta e} = \frac{2n}{\lambda} \Delta v_{\Delta e} \sin\left(\frac{\theta}{2} + \gamma\right)$$

Expressing the broadening as the bandwidth in percent gives

$$\frac{\Delta f_{\Delta e}}{f} = \frac{\frac{2n}{\lambda}\left[2v \cos\left(\frac{\theta}{2} + \psi\right) \sin \gamma\right] \sin\left(\frac{\theta}{2} + \gamma\right)}{\frac{2n}{\lambda} v \sin \frac{\theta}{2}} \tag{7}$$

which reduces to (assuming sin γ is very small)

$$\left(\frac{\Delta f}{f}\right)_I = \cos\left(\frac{\theta}{2} + \psi\right) 2\gamma \tag{8}$$

4.2.2 Type II Broadening

With reference to Fig. 8, Type II broadening is due to the f-numbers of the respective beams. Substituting these limits on θ into the Doppler equation gives

$$\Delta f = \frac{2n}{\lambda} v\left[\sin\left(\frac{\theta + \alpha + \beta}{2}\right) - \sin\left(\frac{\theta - \alpha - \beta}{2}\right)\right]$$

Dividing by f_D to obtain the bandwidth and letting $\frac{\alpha}{2} + \frac{\beta}{2} = \gamma$ give

$$\left(\frac{\Delta f}{f_D}\right)_{II} = \frac{\sin\left(\frac{\theta}{2} + \gamma\right) - \sin\left(\frac{\theta}{2} - \gamma\right)}{\sin \frac{\theta}{2}} \tag{9}$$

which simplifies to

$$\left(\frac{\Delta f}{f_D}\right)_{II} = \frac{2 \cos \frac{\theta}{2} \sin \gamma}{\sin \frac{\theta}{2}} = 2 \operatorname{ctn} \frac{\theta}{2} \sin \gamma \tag{10}$$

By comparing the two broadening effects, it is seen that Type I is always small since the maximum value of $\cos\left(\frac{\theta}{2} + \psi\right) = 1$ and $\sin 2\gamma$ is small compared with $\text{ctn}\left(\frac{\theta}{2}\right)$. Hence

$$\left(\frac{\Delta f}{f_D}\right)_{II} > \left(\frac{\Delta f}{f_D}\right)_{I}$$

This means that Type I broadening is always less than the Type II broadening.

4.3 TRANSIENT DOPPLER DATA

When considering a seed particle traversing the homodyne volume, the corresponding Doppler shifted frequency may be considered as transient data. That is, the seed particle contributes to a pulse of scattered light where the pulse length is determined by the diameter, D, of the homodyne volume and the velocity of the particle. An important characteristic of transient data, as opposed to periodic data, is that a discreet spectral representation, as discussed earlier, is not possible. However, a continuous spectral representation can be obtained for transient data with the use of the Fourier integral given by

$$x(f) = \int_{-\infty}^{\infty} x(t)\, e^{-i2\pi ft}\, dt$$

For further discussion on transient nonperiodic data, see Ref. 2. Several types of transient data will be discussed that represent seed particles traversing the homodyne volume. These are the envelopes of slowly increasing Doppler shifted frequencies for moderate flows and a fast rise of Doppler frequency for high velocities.

Consider first a fast moving particle traversing the scattering volume in such a way that it may be represented by a fast rise time frequency data burst equal to the time it takes to traverse the volume. Therefore,

$$\frac{v}{D} = \frac{1}{\tau} \tag{11}$$

where v is the velocity of the scatter particle, D the diameter of the scattering volume as before, and τ the duration of the square wave. The Fourier transform of this square wave, integrated from $-\tau/2$ to $+\tau/2$ provides the familiar solution of

$$X(f) = \int_{-\tau/2}^{\tau/2} x(t)\, e^{-i2\pi ft}\, dt = A\,\frac{\sin \pi f \tau}{\pi f \tau} \tag{12}$$

where A is a constant. From Eq. (12), it is seen that a minimum is reached for $f = \frac{n}{\tau}$ and n = 1, 2, 3, ... Since electronic instrumentation generally is concerned with the power frequency spectrum, the resulting display is represented by an amplitude-frequency plot shown in Fig. 9. This resulting frequency broadening may then be approximated at the half power point by Δf relative to the time a scatter particle spends in the scatter volume. That is,

$$\frac{v}{D} = \frac{1}{\tau} \simeq \Delta f \tag{12a}$$

Hence, from Eqs. (11) and (12), it is seen that the frequency broadening is minimized by making τ large such that the oscillations of X(f) increase since the cross-over points $\frac{n}{\tau}$ approach the origin. That is, the Doppler frequency f_o contained in the square wave burst approaches the bandwidth of the instrument when $\tau \to \infty$ as is effectively the case in the top trace in Fig. 2 and represented graphically in the last part of Fig. 9. This may be accomplished by making the scattering volume, D, large in order to make this frequency broadening small.

A particle moving slowly through the scatter volume may have a Gaussian-type curve as an envelope of the Doppler frequency. Fourier transforms of this type distribution are similar to the transform of the square wave previously discussed (Ref. 3). The bandwidths Δf of the center portion of the transformed frequency envelopes are similar in that they tend to decrease in Δf as the data curve becomes broader. Figure 9 illustrates this point. Conversely, the Δf becomes broader if the envelope of the data curve is narrow (small variance) as is the case for small scatter volumes. Hence, a fractional bandwidth is associated with data burst, which may be expressed as

$$\left(\frac{\Delta f}{f_D}\right)_t = \frac{v/D}{\frac{nv}{\lambda}\sin\theta} = \frac{\lambda}{nD\sin\theta} \tag{12b}$$

4.4 FREQUENCY MODULATION

In some cases where the scattering volume is small and sufficient seeding is present, the Doppler shifted laser frequency, originating from the ensemble of scattering particles, may add in phase in such a way as to provide an almost continuous in time, Doppler shifted frequency. Longitudinal velocity gradients would contribute to a frequency modulation of the detected Doppler frequency. This frequency modulation may be expressed as

$$m_f = \frac{\text{frequency deviation}}{\text{modulation frequency}} = \frac{\Delta f}{f} \tag{13}$$

where m_f may be termed the modulation index (Ref. 4). The power spectrum of these expanding and contracting sine waves, about the mean frequency, f_o, contribute to broadening of the power spectrum by frequency components spaced by the modulating frequency and having amplitudes expressed by Bessel functions of the first kind and nth order, with argument m_f, the modulating index. A graphical representation of the broadening of the power spectrum is shown in Fig. 10 where the effects of constant modulation frequency versus an increasing frequency deviation are illustrated. In addition, the effects of a variable modulation frequency on a constant frequency deviation are also illustrated. As the modulation frequency increases, more frequency components are added between the already existing spectra. That is, the spectra becomes more continuous, not broader, with increasing modulation frequency. From Fig. 10, it is seen that, in extreme cases of frequency deviations (longitudinal velocity gradients), no significant information may be obtained from the power frequency spectrum of a spectrum analyzer.

4.5 BROWNIAN MOTION

4.5.1 Particle Fluctuation

The random motion of molecules of either liquid or gases bombard suspended particles in a more or less random way such that particles moving along a stream line are constantly being influenced by their surrounding medium. This, therefore, requires some knowledge to the degree of the effect the surrounding molecules have on the laser velocimeter readings. Since inferences are made from knowing the particle motion, the surrounding medium motion is implied.

These random fluctuations of the particles are manifested as variations about the mean velocity of the particles such that a broadening effect is seen as displayed on a spectrum analyzer.

The distribution of the fractional number of particles with velocity v_x to $v_x + dv_x$ has been derived in great detail elsewhere (Ref. 5) and may be written as

$$\left(\frac{dN}{N}\right)_{vx} = \left(\frac{m}{2\pi kT}\right)^{1/2} \exp\left(\frac{-m v_x^2}{2kT}\right) dv_x \equiv f(v_x)\, dv_x \qquad (14)$$

for particle velocity components in the x-direction only. [2]

[2]Here, interest is only with velocities in the x-direction. If the other two components are summed with $f(v_x)$, the familiar Maxwell-Boltzmann distribution results.

The function, $f(v_x)$, is clearly a Gaussian distribution with increasing variance as temperature, T, increases.

In order to determine the fractional bandwidth, $\frac{\Delta f}{f_D}$, about a mean velocity of v_o, Eq. (14) is written as

$$dv_x f(v_x) = \left(\frac{m}{2\pi kT}\right)^{1/2} \exp\left[\frac{-m(v_x - v_o)^2}{2kT}\right] dv_x$$

The maximum value of this function occurs at $v_x = v_o$, so

$$f(v_x)_{max} = \left(\frac{m}{2\pi kT}\right)^{1/2} \tag{15}$$

The half value points occur at $\frac{f(v_x)_{max}}{2}$ such that it is possible to solve for $(v_x)_{1/2}$.

$$\frac{f(v_x)_{max}}{2} = \left(\frac{m}{2\pi kT}\right)^{1/2} \exp\left[\frac{-m(v_x - v_o)^2}{2kT}\right] = \frac{1}{2}\left(\frac{m}{2\pi kT}\right)^{1/2} \tag{16}$$

or

$$1 = 2 \exp\left[\frac{-m(v_x - v_o)^2}{2kT}\right]$$

Taking the log on both sides and regrouping terms give

$$v_x^2 + (-2v_o) v_x + \left[v_o^2 - \frac{2kT}{m} \ell n\, 2\right] = 0$$

which is in standard quadratic form giving the two velocities at the half value point.

$$v_{1,2} = v_o \pm \sqrt{(2kT/m) \ell n\, 2} \tag{17}$$

Let

$$\Delta v_x \equiv v_1 - v_2 = v_o + \sqrt{(2kT/m) \ell n\, 2} - v_o - \sqrt{(2kT/m) \ell n\, 2}$$

or

$$\Delta v_x = \sqrt{(8kT/m) \ell n\, 2} \tag{18}$$

Equation (18) shows that the half width is independent of the mean velocity of the fluid. This statement was certainly true. From the velocimeter equation, Eq. (2), the velocity is directly proportional to frequency, such that

$$\frac{\Delta v_x}{v_o} = \frac{\Delta f}{f_D} = \frac{1}{v_o} \sqrt{(8kT/m) \ell n\, 2} \tag{19}$$

Equation (19) shows the fractional bandwidth as being very negligible for particles much heavier than the molecules, especially for increasing mean velocities, v_o.

A typical example may be illustrated for 1-μm particles with mean velocity of 1 meter/sec. By taking the temperature to the T = 300°K and the remaining parameters as k = 1.38 x 10^{-23} joules/K° and mass (m) = 10^{-15} kg,

$$\frac{\Delta f}{f_D} = \left[\frac{8 \times 1.38 \times 10^{-23} (300)(0.693)}{10^{-15} (1)}\right]^{1/2} = (23 \times 10^{-6})^{1/2}$$

$$\frac{\Delta f}{f_D} \approx 0.005$$

For increased temperature and lower velocities, the broadening effect may be significant, but in most cases, an increased temperature generally implies an increased velocity, as in rocket exhausts, turbojets, etc.

4.5.2 Concentration Fluctuations

In perfectly homogeneous solutions and in the absence of impurities, no light scattering is observed. But in real solution, it is found that the random diffusive motion of the fluid causes spontaneous formation of concentration fluctuations. The concentration fluctuations are manifested as small changes of the index of refraction due to the variation in the dielectric constant of the fluid. This causes the fluid to act as a random scattering center above and beyond any residual solid light scatterer in the fluid.

These arbitrary concentration fluctuations may be analyzed by Fourier analysis such that they may be thought of as linear combinations of sinusoidal concentration waves. Therefore, the observed light scattering at any point is due to constructive interference of reflected light waves.

Let the wave vectors of the incident and scattered light be $\bar{k}_o$ and $\bar{k}_s$, respectively (the same wave vectors as for the LDV), then the familiar Bragg condition (Ref. 7) may be written as

$$\bar{K} = \bar{k}_s - \bar{k}_o \tag{20}$$

where $\bar{K}$ is the wave vector associated with the light scattering due to the fluctuation. A vector diagram of ($\bar{k}_S$ - $\bar{k}_O$) will immediately show that the magnitude of $\bar{K}$ is

$$K = 2k_o \sin \theta/2 \tag{21}$$

Since $\left|\bar{k}_o\right| = \left|\bar{k}_s\right| = \frac{2\pi}{\lambda}$, the same as in the analysis of the LDV. Since K is the wave vector associated with the fluctuation, its magnitude is $K = \frac{2\pi}{\Lambda}$, where Λ is the wavelength of Fourier component of the fluctuation causing the scattering.

Equation (21) may then be written as

$$\frac{2\pi}{\Lambda} = 2\left(\frac{2\pi}{\lambda}\right) \sin \theta/2$$

or

$$\lambda = 2\Lambda \sin \theta/2 \tag{22}$$

This equation indicates that, for small θ, longer fluctuation (large amplitude) are required to produce scattering of light. To determine the magnitude of these fluctuations, especially their frequency distribution, this scattering phenomena must be considered as a random process in time. It is assumed here and by others (Ref. 6) that the well known random walk problem applies to this analysis. Thus since the electric field strength of the scattered light is proportional to the fluctuation of the dielectric constant, the power spectrum of these fluctuations may be determined with the use of the Wiener-Khintchine (Fourier-transform) theorem,

$$G(\omega) = 4 \int_o^\infty R_E(\tau) \cos 2\pi f\tau \, d\tau \tag{23}$$

where $R_E(\tau)$ is the autocorrelation function which is characterized by the product of electric field $E(\tau)$ time averaged over the ensemble, ω is given by $\omega = 2\pi f$, and τ is a time slightly different than t. Thus $R_E(\tau) = <E^*(t)E(t + \tau)>$. It can be shown (Ref. 6) that

$$R_E(\tau) \propto \exp\left(-2\omega_o\tau - Dk^2|\tau|\right) \tag{24}$$

which is derived from the random walk problem, where D is the diffusion constant. The diffusion constant, D, is expressed by the Einstein relation which states that

$$D = kT \cdot \text{mobility}$$

where the mobility is defined as the concentration drift velocity per unit force. For concentration fluctuations, the diffusion coefficient is determined by Fick's first law, mathematically stated as

$$J_x = -D \frac{\partial C(x,t)}{\partial x}$$

where C(x, t) is the concentration function being expressed as a Gaussian distribution varying in time and distance in a given direction.

The range over which the diffusion coefficient varies in a liquid is found experimentally to lie between 10^{-4} and 10^{-6} cm^2/sec (Ref. 7). The scattered wave vector k comes into Eq. (24) through the Fourier component phase relation of scattered light due to the concentration fluctuation. Substituting Eq. (24) into Eq. (23) yields the power spectrum,

$$G(\omega) \propto \frac{DK^2}{(\omega - \omega_o)^2 + (DK^2)^2} \tag{25}$$

which is in the form of a Lorentzian distribution. The power spectrum is seen to center around ω_o, the laser light frequency. At half maximum of the Lorentzian distributing, the frequency bandwidth encompassed by the half power points, letting $\Delta\omega \equiv (\omega - \omega_o)$, is clearly

$$\Delta\omega = 2DK^2 \tag{26}$$

Since

$$\Delta\omega = 2\pi\Delta f$$

then

$$(\Delta f)_{1/2} = \frac{DK^2}{\pi} \tag{27}$$

The heterodyning technique employed in laser velocimetry shifts this distribution around the frequency associated with the velocity, i. e., $f_D = \overline{K} \cdot \overline{v}$ or Eq. (2).

Equation (27) expresses this frequency distribution in terms of the diffusion constant and the scattering vector. A typical example for LDV application, $(\Delta f)_{1/2}$ in liquids is found to be less than 600 Hz for a scattering angle of 10 deg. The diffusion coefficient was taken to be 10^{-4} cm^2/sec. Studies of the temperature dependence of the diffusion coefficient of liquids generally leads to an empirical relationship of the form $D = D_o \exp -(Q/RT)$ (Ref. 7), where D_o and Q are experimental parameters that are essentially temperature dependent and characteristic of the system under study. As has been suggested by others (Ref. 7), the diffusion coefficient may be determined by Eq. (27) since other experimental determination of D is a difficult and time-consuming process.

Clearly the smaller the scattering angle θ, the smaller the frequency broadening effect. Also, the autocorrelation function $R_E(\tau)$ suggests a correlation time $\tau_C = \frac{1}{DK^2}$ associated with these fluctuations. Here, there is an increase in correlation time with small scattering angle θ. This may be observed experimentally by observing the characteristic twinkling about a laser beam passing through a liquid

and impinging on a screen. One sees the intensity fluctuation to greatly decrease, along with an increase in the average spot size (coherence area) when observations are made with small scattering angles. Conversely, greater scattering angles, as seen on the periphery of the screen, increases the fluctuation frequency with a decrease in the average coherence area.

SECTION V
SUMMARY AND CONCLUSION

The laser Doppler velocimeter provides velocity data from a small volume determined by the geometry of the lens-beam diameter combination and to the extent of the diffraction limit of the laser and lens. Since the focal volume is finite, a velocity distribution will be obtained when velocity fluctuations, as seen in turbulence, are present. This velocity distribution is manifested in the frequency analysis such that factors contributing to the frequency distribution must be readily understood. Considerable efforts are being directed toward automated, continuous sampling of Doppler shifted data, and since all frequency broadening effects may be displayed on a frequency spectrum analyzer, any discrepancies between the two methods may be understood better by studying the spectrum analyzer data. A report is being prepared discussing the relation between an automated frequency readout and frequency spectrum analyzers.

An overall summary of the frequency broadening is presented in tabular form in Table II. It is seen that all, except one, of the broadening effects have their true velocity presented at the maximum intensity of the distribution density function as does the presentation of a spectrum analyzer. The size of the volume in which velocity information is estimated does not necessarily limit the accuracy of the measurement. The error in the LDV system lies in the determination of the maximum intensity of the distribution density function with increasing error as the bandwidth increases. In the way of illustration, Foreman, et al (Ref. 8), estimated that a bandwidth of 20 percent would allow the maximum intensity to be determined within ±3 percent.

The frequency broadening originating from finite probe volume size was seen to be quite drastic in the boundary layer. This problem may be made small by making certain that the light scattering collecting lens is appropriately apertured for limited light collection. As seen from the photographs, an accurate determination of f_o is not difficult and may easily be determined within 5 percent. The experimentally

observed skewness of frequency peaks has been traced to a variation of the velocity gradient in the scattering volume.

In the discussion of transient data, it was found that a large probe volume makes $1/\tau$ small, which contributes to narrower frequency peaks.

The effect of the Δk_s and Δk_o variations is also seen to be a significant contributor to frequency broadening when the standard optics arrangement (shown in Fig. 3) is used. Alternate optics arrangements have been successfully utilized for minimizing this effect.

The effect of frequency modulation is thought to be a small contributing factor in velocimetry. In water flows, a longitudinal velocity gradient may cause momentary loss of spectrum analyzer signal if the frequency deviations are large. An adequate filtering technique can almost eliminate this problem; however, it has been observed that in gas flows, similar velocity gradients also occur, and momentary signal drop-out becomes a problem in velocity measurements of gaseous media.

The temperature broadening associated with Brownian motion may be considered negligible at STP, except at very low mean velocities and very small particle sizes. An experiment was set up to measure the concentration fluctuations in liquids with no success. Since the correlation time τ_C was very small, the spectrum analyzer was unable to produce this broadening even with the slowest scan speed of the instrument.

REFERENCES

1. Snyder, W. T. and Goethert, W. H. "Experimental Investigation of Laminar Flow Development in a Rectangular Channel Using a Laser Anemometer." AEDC-TR-69-186 (AD695032), October 1969.

2. Bendat, J. S. and Piersol, A. G. Measurement and Analysis of Random Data. Wiley, New York, 1966.

3. Jenkins, F. A. and White, H. E. Fundamentals of Optics. McGraw-Hill, New York, 1957, Third Edition.

4. Bracewell, R. The Fourier Transform and its Application. McGraw-Hill, New York, 1965.

5. Sears, F. W. Thermodynamics. Addison-Wesley Publishing Co., Inc., Second Edition, 1959.

6. Clark, N. A. and Lunacek, J. H. "A Study of Brownian Motion Using Light Scattering." American Journal of Physics, September 1969.

7. Adler, R. "Interaction Between Light and Sound." IEEE Spectrum, May 1967.

8. Foreman, J. W., et al. "Laser Doppler Velocimeter for Measurement of Localized Flow Velocities in Liquids." Proc. IEEE 54, 1966.

APPENDIXES
I. ILLUSTRATIONS
II. TABLES

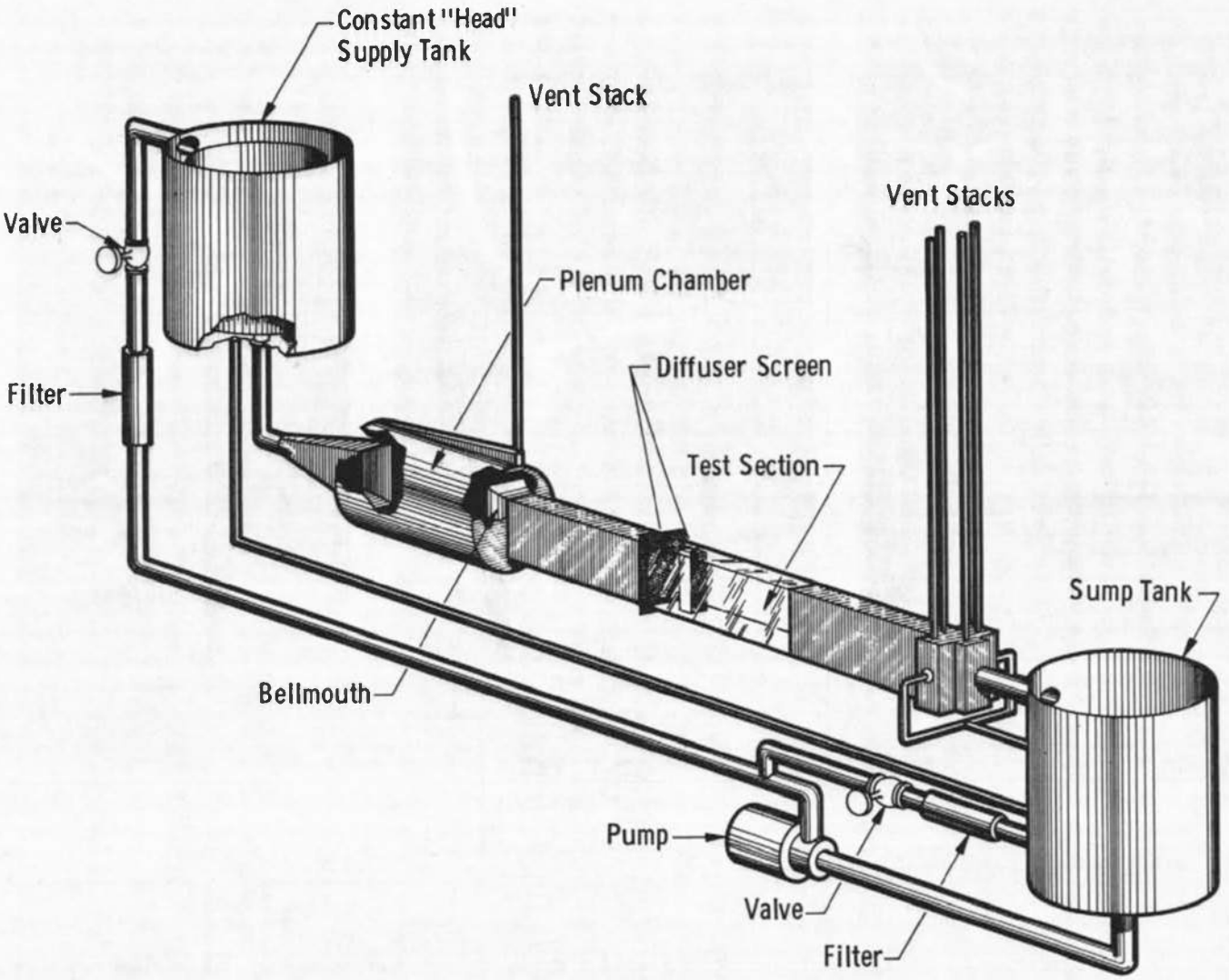

Fig. 1 Schematic Diagram of Flow System

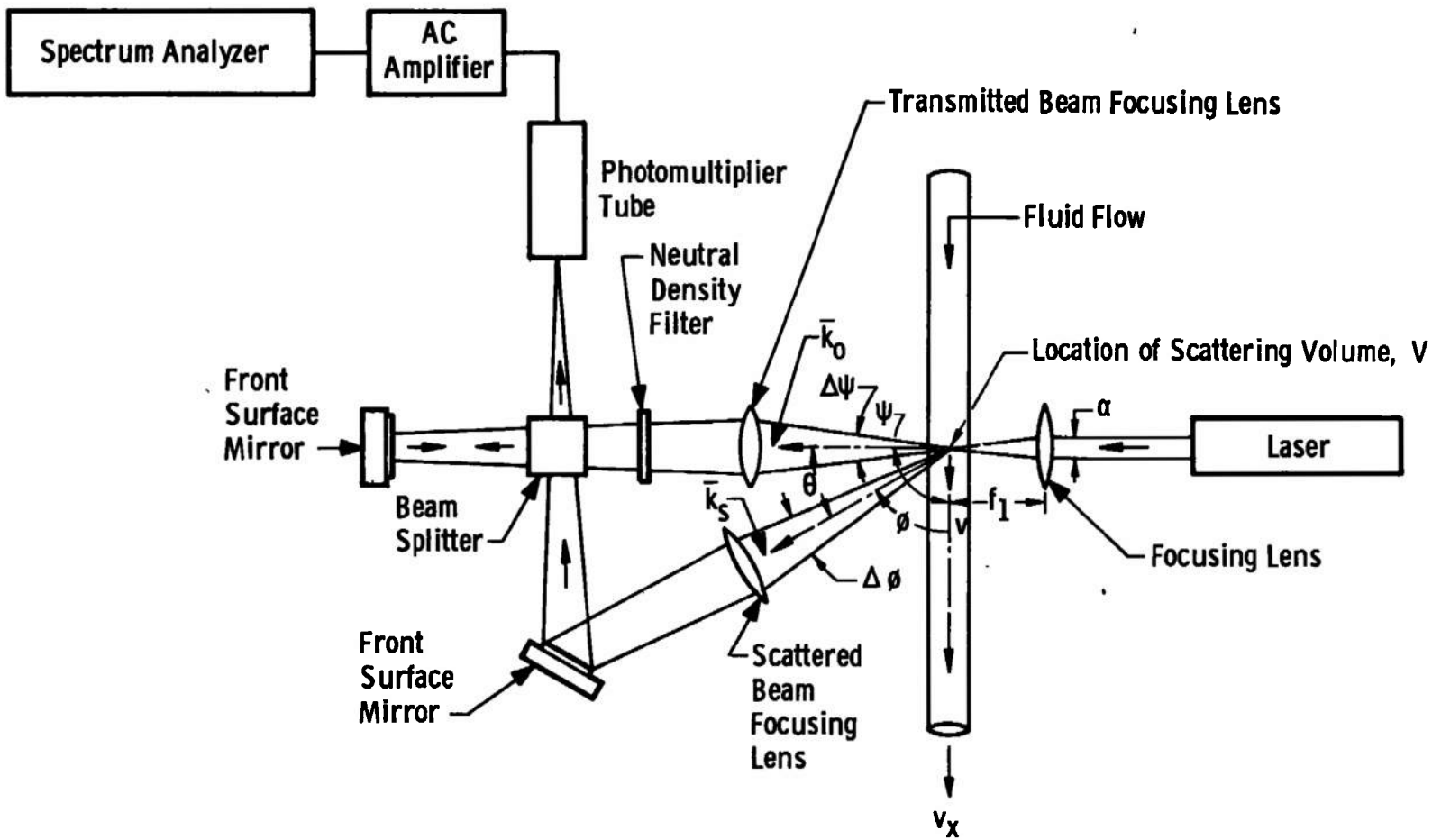

Fig. 2 Setup of the LDV on the Water Flow System

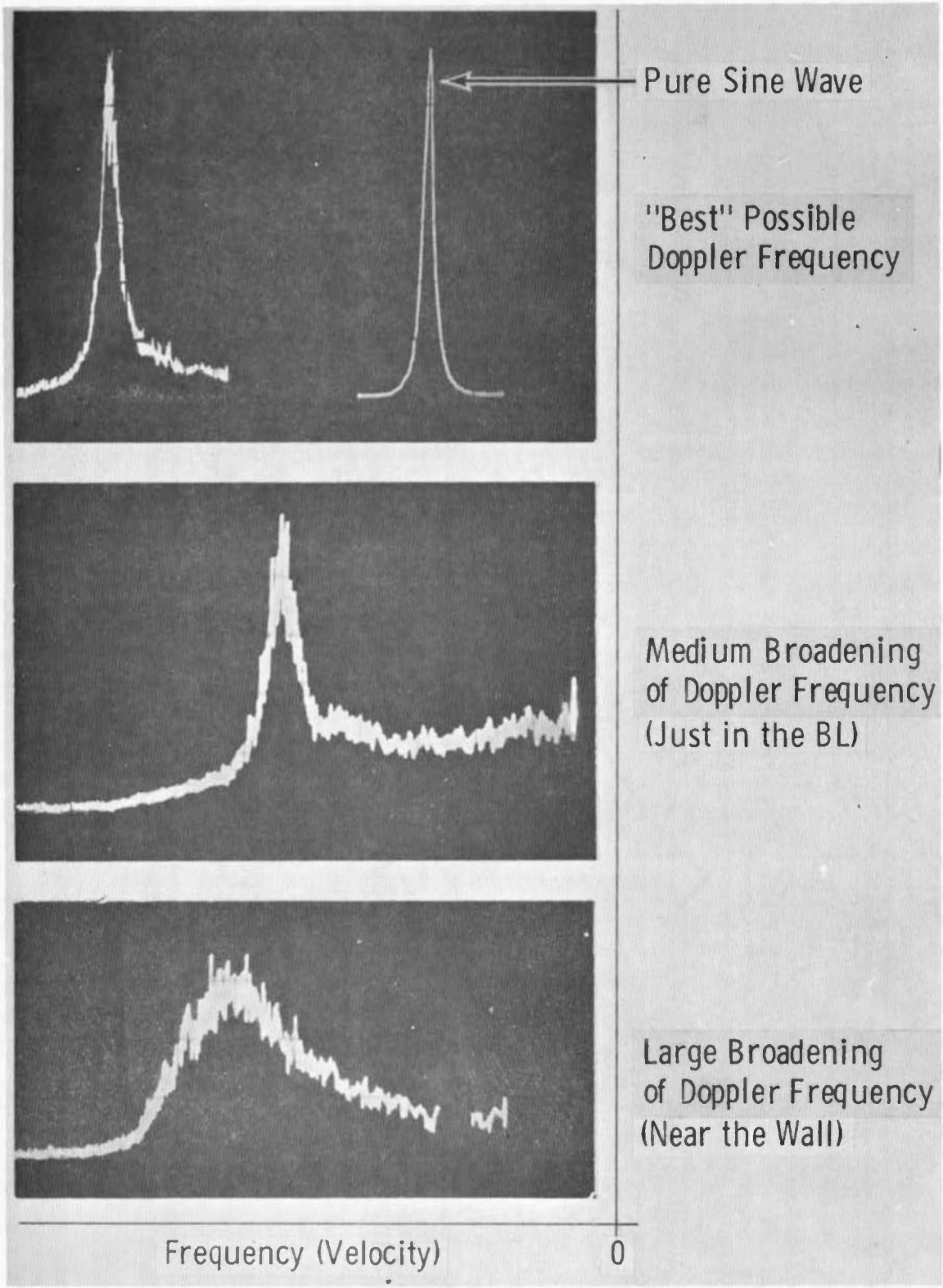

Fig. 3 Frequency Broadening at Constant Settings of Readout Instrument at Various Stations of the Channel Flow

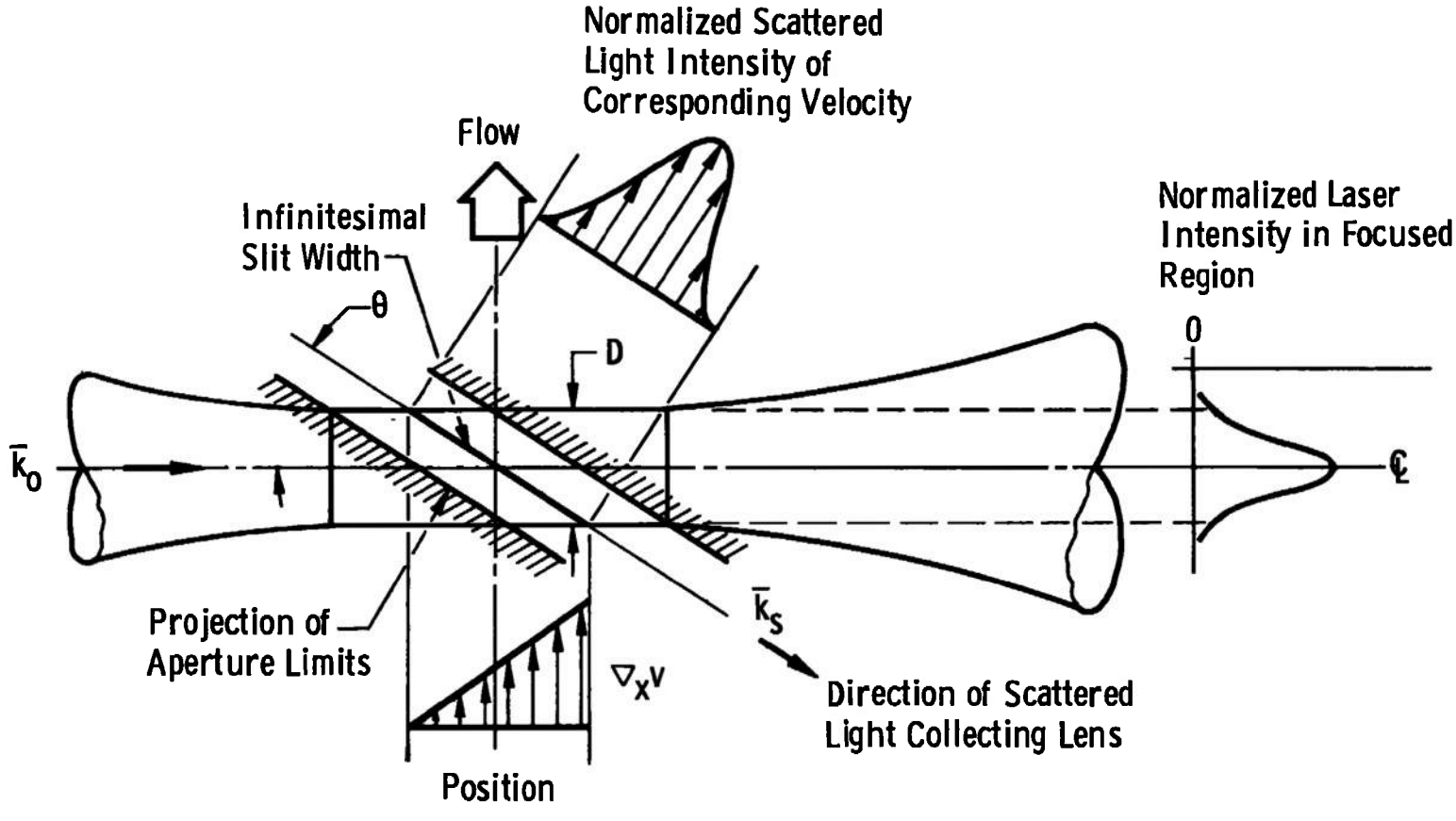

Fig. 4 Model of Scattering Volume

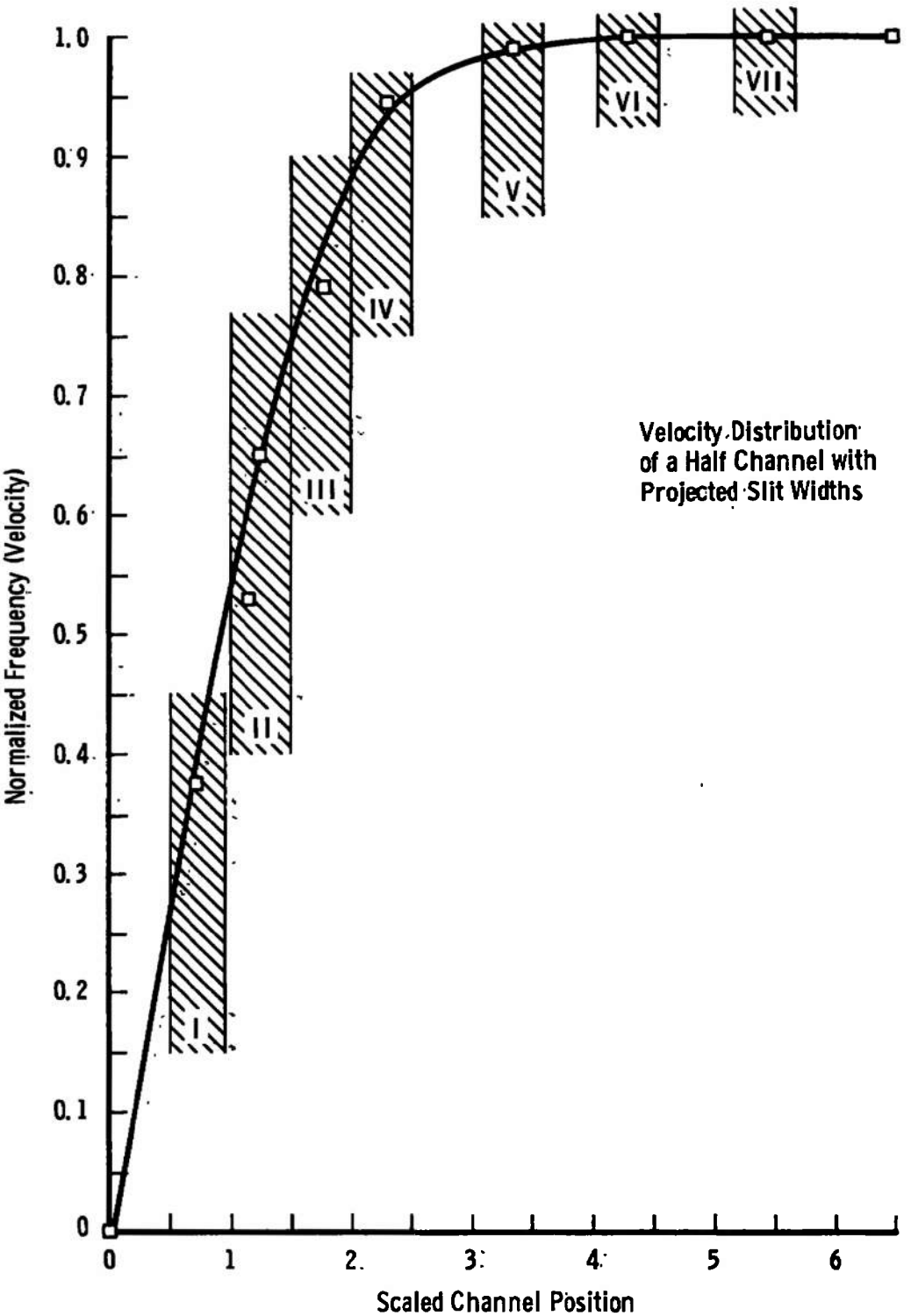

Fig. 5 Normalized Velocity Profile

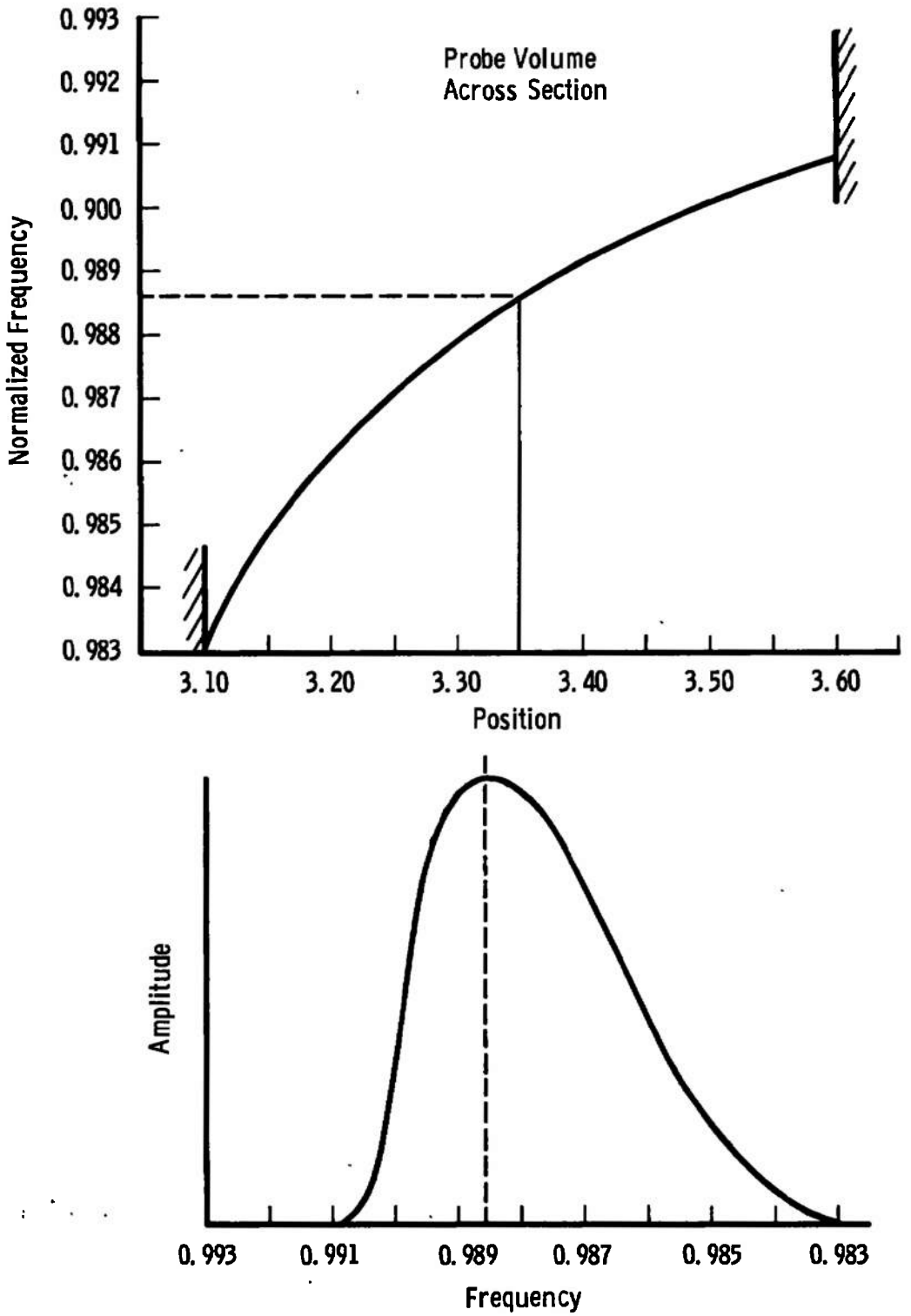

a. Nonlinear Velocity Gradient Projected into the Frequency Domain

Fig. 6 Velocity Gradient Projection

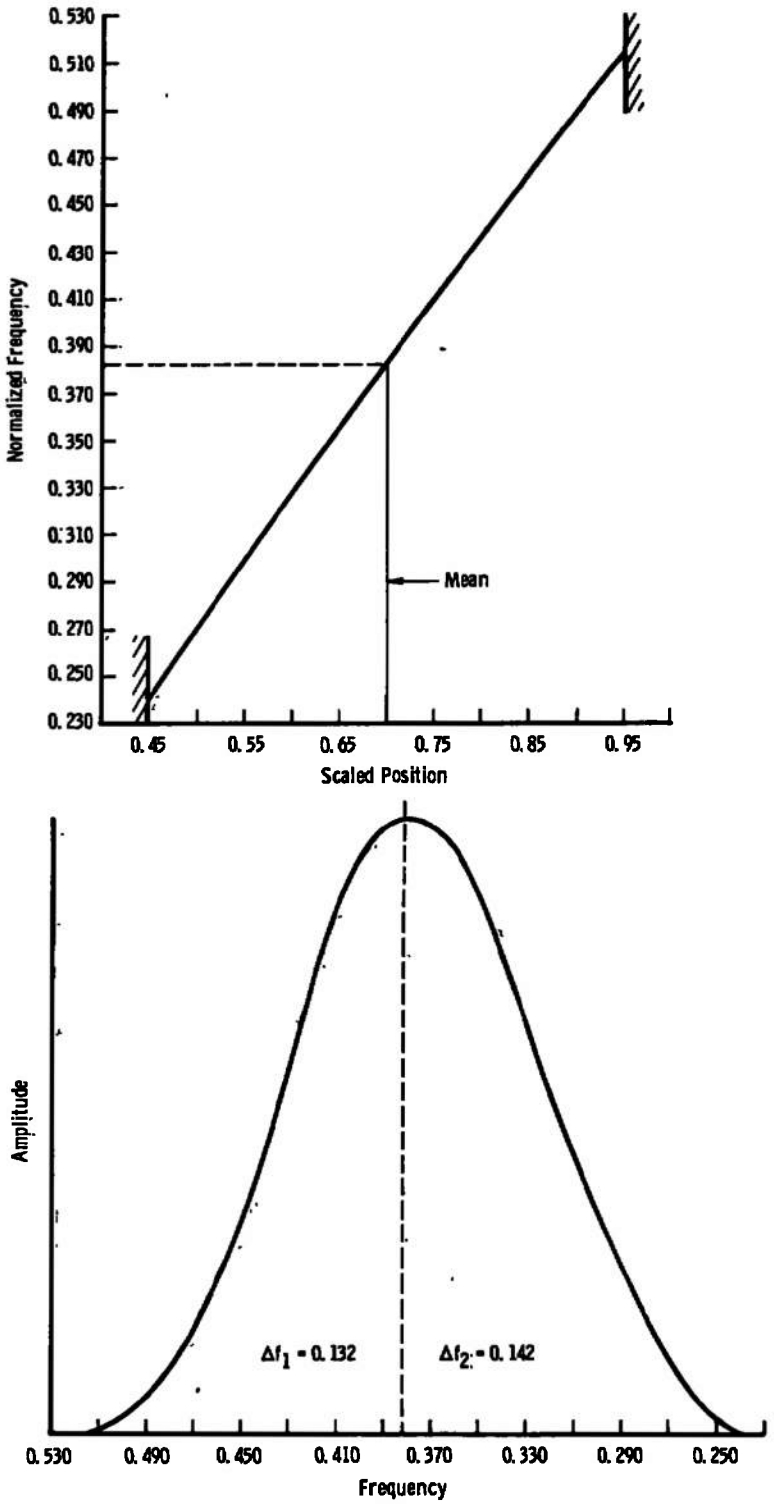

b. Almost Linear Velocity Gradient Projected into an Almost Gaussian Frequency Distribution

Fig. 6 Concluded

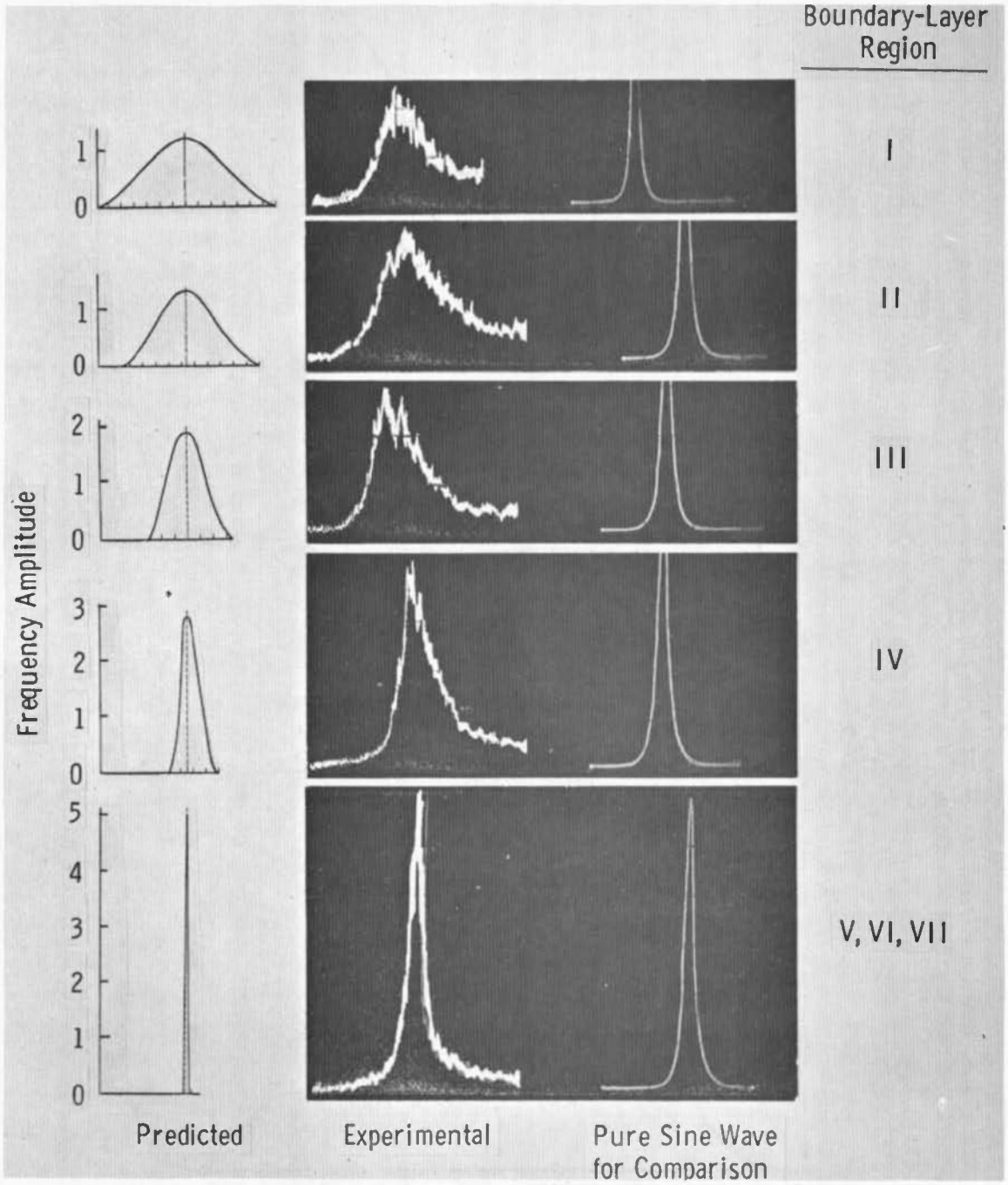

Fig. 7 Boundary-Layer Frequency Distribution

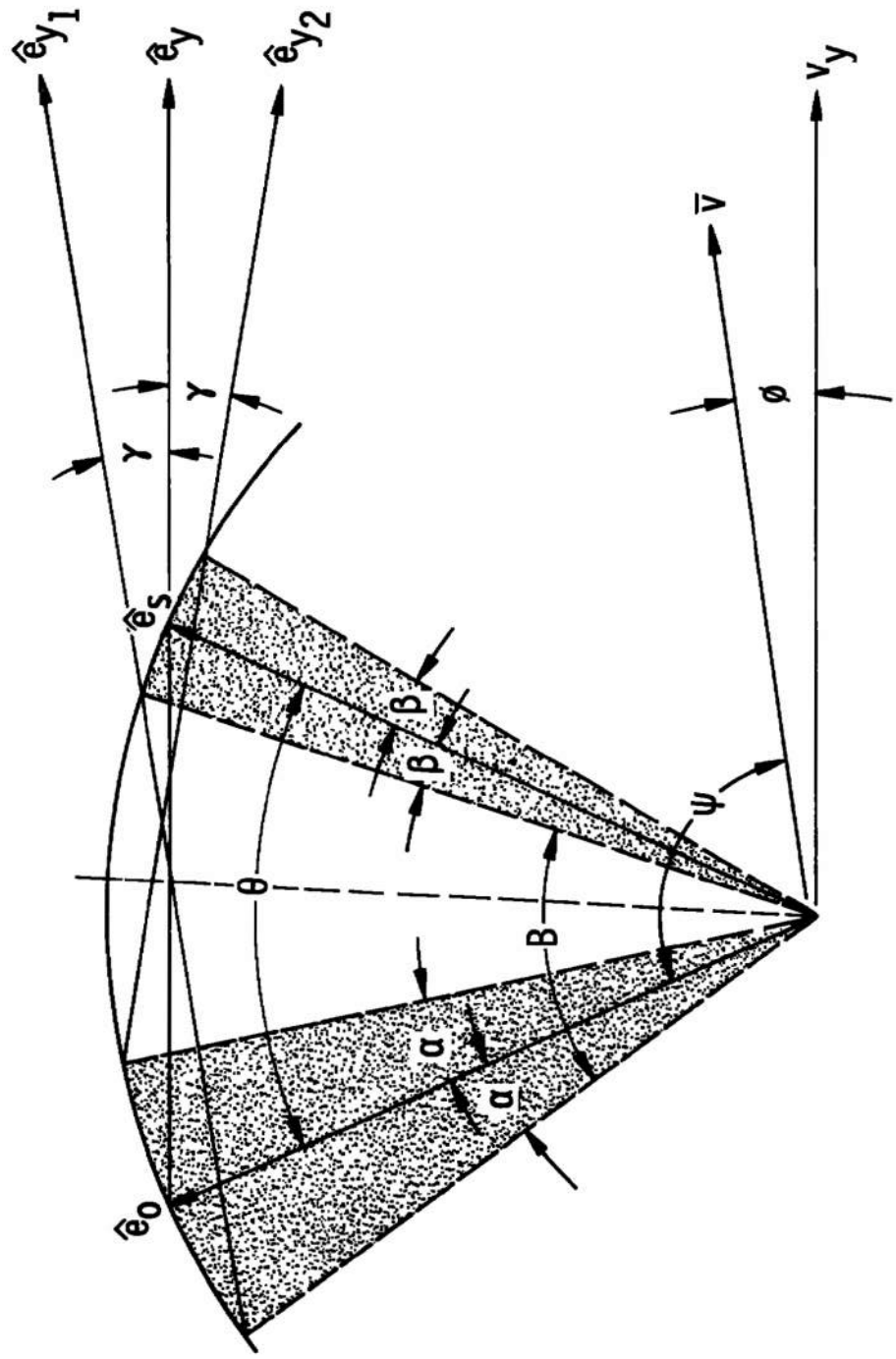

Fig. 8 Vector Representation of the Velocity Measurement

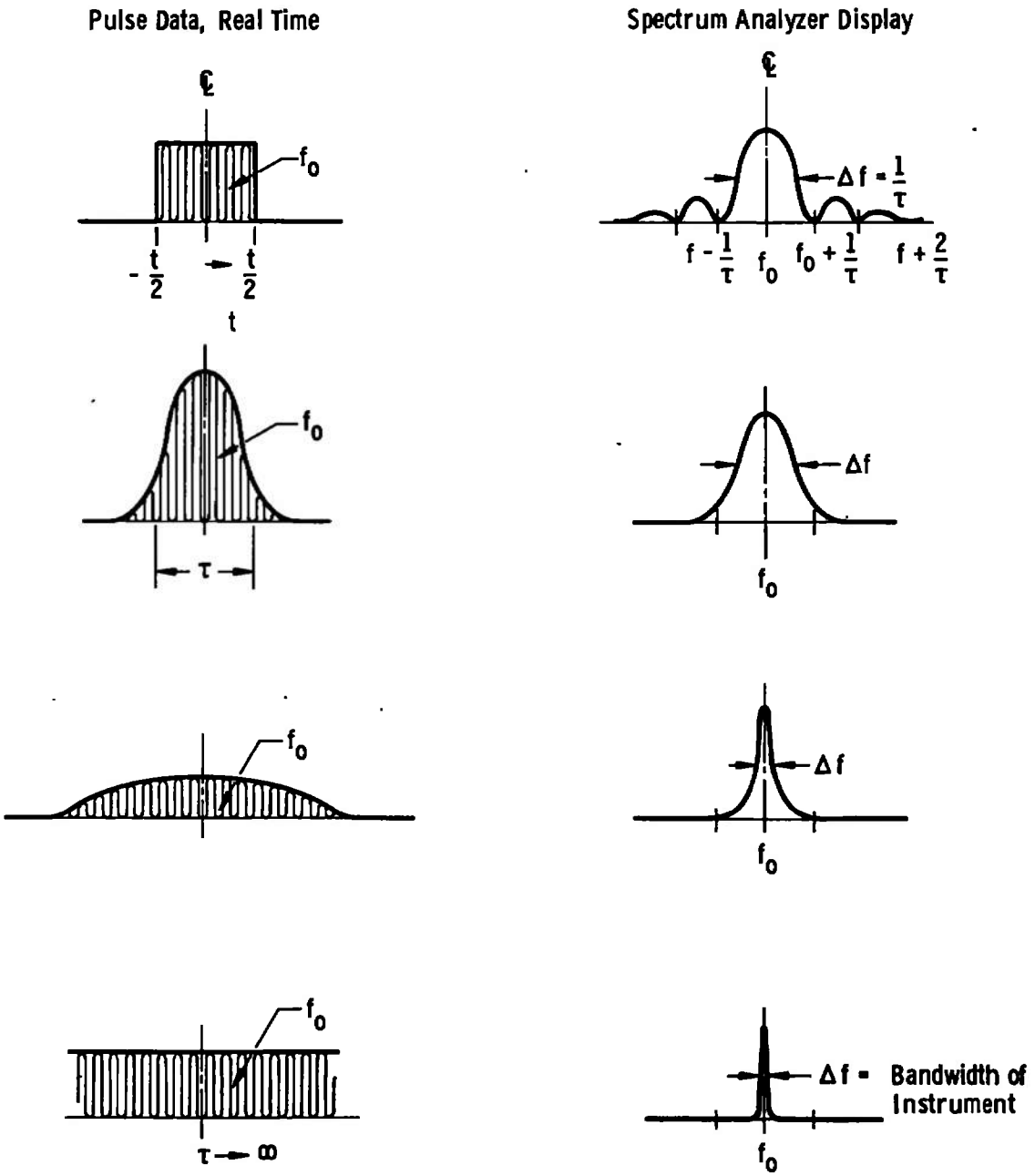

Fig. 9 Amplitude-Frequency Variation

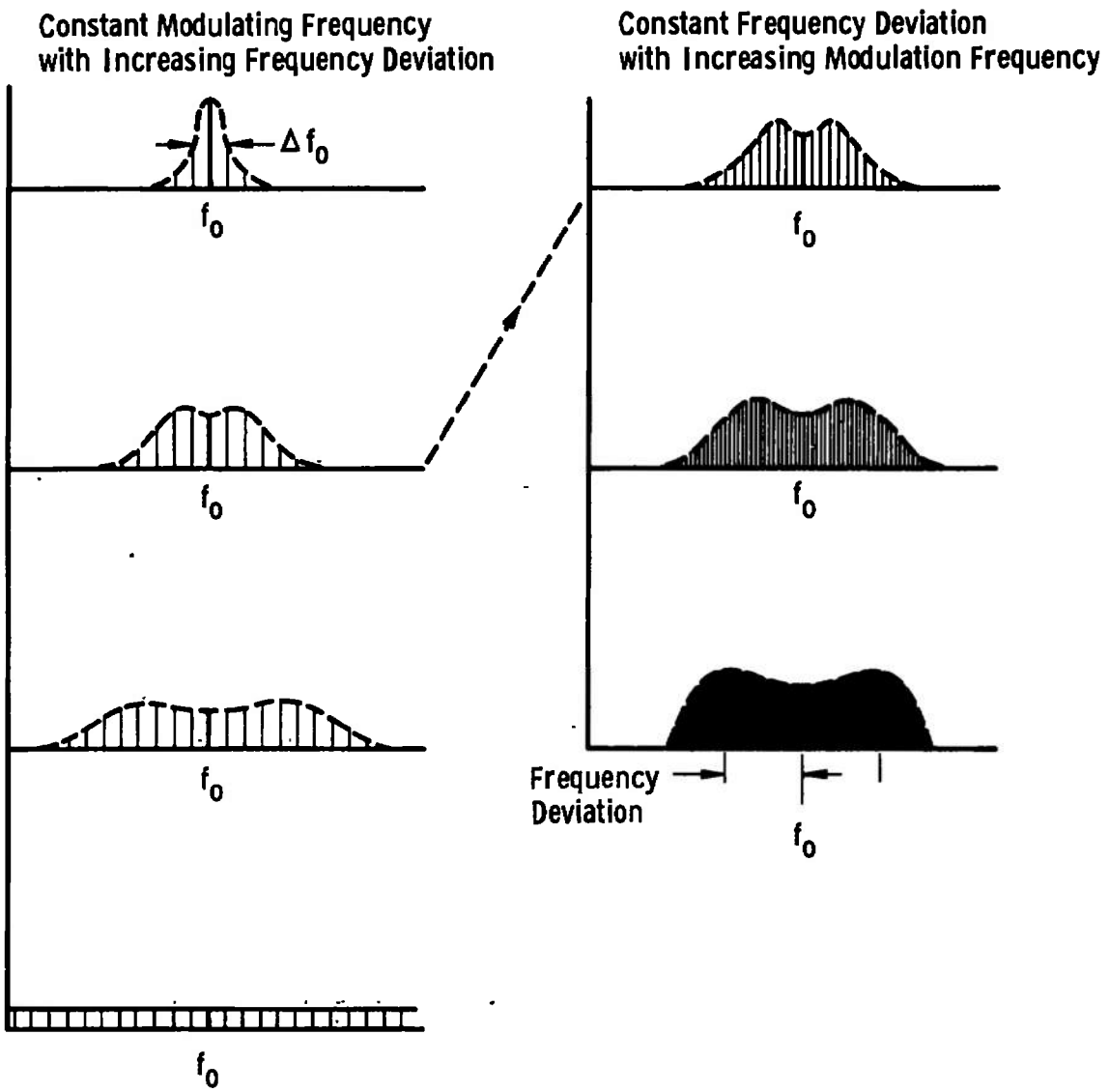

Fig. 10 Effects of Frequency Modulation

TABLE I
CALCULATED AND EXPERIMENTAL MAXIMUM INTENSITY

$f(v)_{max} \propto k/b$ with $k = 1(ft/sec) \cdot (cm)$ and $b = V_{max} - V_{min}$

	Calculated from finite aperture		Photographs
Fig. 5	k/b	ℓn k/b	$\ell n(f)$ = Ampl. in cm
I	3.75	1.32	1.4
II	4.35	1.47	1.6
III	7.7	2.04	1.9
IV	21.2	3.05	2.8
V, VI, VII	201.0	5.29	4.4

TABLE II
SUMMARY OF BROADENING EFFECTS

Type	Sym.	Skewness Toward	True Velocity at Maximum Intensity*
$\Delta\hat{e}_y$	No	Low	Yes
grad. v_x	No	Low	Yes
$\Delta\theta$	Yes	None	Yes
Instrument Analyzer	Yes	None	Yes
Pulse	Yes	None	Yes
$\frac{\partial v}{\partial t}$	Yes	None	No
Temperature (Brownian)	Yes	None	Yes

*"True" velocity is taken as the recorded data point corresponding to the geometrical center of the probe volume. Maximum intensity refers to the greatest value of the distribution density function.

UNCLASSIFIED

Security Classification

DOCUMENT CONTROL DATA - R & D

(Security classification of title, body of abstract and indexing annotation must be entered when the overall report is classified)

1 ORIGINATING ACTIVITY (Corporate author) Arnold Engineering Development Center, ARO, Inc., Operating Contractor, Arnold Air Force Station, Tennessee 37389	2a. REPORT SECURITY CLASSIFICATION UNCLASSIFIED 2b. GROUP N/A

3 REPORT TITLE

FREQUENCY BROADENING IN REFERENCE BEAM LASER DOPPLER VELOCIMETER DATA

4 DESCRIPTIVE NOTES (Type of report and inclusive dates)

Final Report

5. AUTHOR(S) (First name, middle initial, last name)

W. H. Goethert, ARO, Inc.

6 REPORT DATE September 1971	7a. TOTAL NO OF PAGES 41	7b. NO. OF REFS 8
8a. CONTRACT OR GRANT NO. F40600-72-C-0003 b. PROJECT NO. 4344 c. Program Element 64719F d.	9a. ORIGINATOR'S REPORT NUMBER(S) AEDC-TR-71-163 9b. OTHER REPORT NO(S) (Any other numbers that may be assigned this report) ARO-OMD-TR-71-102	

10. DISTRIBUTION STATEMENT

Approved for public release; distribution unlimited.

11 SUPPLEMENTARY NOTES Available in DDC	12. SPONSORING MILITARY ACTIVITY Arnold Engineering Development Center, Air Force Systems Command, Arnold AF Station, Tenn. 37389

13 ABSTRACT

The laser Doppler velocimetdr (LDV) provides velocity data in the form of a frequency spectrum. Because of the inherent optical geometry of the laser velocimeter and the effects of light scattering particles passing through the probe volume, a frequency distribution density function representing these combined effects is found in the readout device. Hence, interpretation of data must be effected for frequency-to-velocity conversion. This report deals with this frequency broadening effect associeted with the LDV reference beam type. Six frequency broadening effects are discussed in terms of their magnitude and relative importance.

DD FORM 1 NOV 65 1473

UNCLASSIFIED

Security Classification

14. KEY WORDS	LINK A		LINK B		LINK C	
	ROLE	WT	ROLE	WT	ROLE	WT
frequency distribution						
frequency converters						
lasers						
Doppler effect						
speed indicators						